Chemical Bioimaging

DOI: 10.1002/ange.201001560

Quantitative CARS Molecular Fingerprinting of Single Living Cells with the Use of the Maximum Entropy Method**

Masanari Okuno, Hideaki Kano, Philippe Leproux, Vincent Couderc, James P. R. Day, Mischa Bonn, and Hiro-o Hamaguchi**

Vibrational spectra are often called "molecular fingerprints". Once vibrational spectra are obtained for the so-called fingerprint region (between 1800 cm^{-1} and 800 cm^{-1}), which exhibits many skeletal vibrations that are highly sensitive to molecular structure, we can derive detailed and otherwise unobtainable molecular information from any kind of material systems ranging from a molecule to a living cell. Since biological systems are made up of molecules, vibrational spectroscopy should be useful in life/biological sciences as much as it is in material sciences. For biological applications, Raman spectroscopy is more suitable than infrared spectroscopy, because it is not seriously influenced by water, which has very strong absorption in the infrared region. Raman spectroscopy is more advantageous than infrared also in space-resolved experiments under a microscope. Raman spectroscopy can achieve sub-micrometer spatial resolution by using a confocal optical microscope but infrared can only manage spatial resolution of a few micrometers because of the diffraction limit. Thus, Raman spectroscopic techniques, both linear and non-linear, have been extensively used for measuring vibrational spectra and images of biological systems under a microscope.[1–6] Among these, coherent anti-Stokes Raman scattering (CARS) microscopy has been a technique of focus for high-speed vibrational imaging.[1–3,7–9] This technique employs a set of two narrow-band laser lines (ω_1 and ω_2) for exciting an isolated and intense Raman band (generally the CH stretch band) to obtain a vibrational image. However, current CARS microscopy is difficult to apply to the fingerprint region, where many Raman bands are located very close to one another. It is lacking in spectral coverage and resolution, which are needed for separating bands in the congested fingerprint region.

Herein, we extend CARS microscopy to CARS microspectroscopy by "spectral imaging"; we used a straightforward spectral analysis to extract quantitative vibrational information from congested vibrational spectra and map out specific molecular moieties within a cell. We used the multiplex CARS method[10–13] (Figure 1a) for obtaining

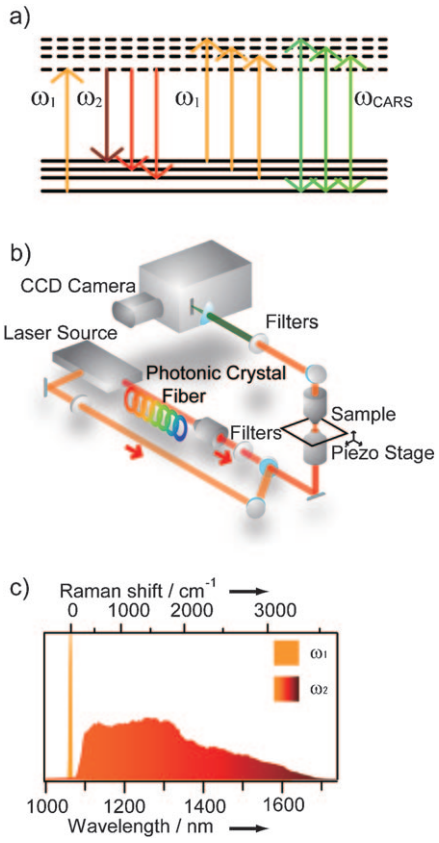

Figure 1. Principle and design of an ultrabroadband multiplex CARS microspectrometer for molecular fingerprinting. a) Multiplex CARS process; b) experimental setup; c) spectra of the ω_1 and ω_2 radiation (intensity uncorrected).

[*] M. Okuno, Prof. Dr. H. Kano, Prof. Dr. H. Hamaguchi
Department of Chemistry, School of Science
The University of Tokyo
Hongo 7-3-1 Bunkyo-ku Tokyo, 113-0033 (Japan)
Fax: (+81) 3818-4621
E-mail: hhama@chem.s.u-tokyo.ac.jp

Prof. Dr. H. Hamaguchi
Institute of Molecular Science, National Chiao Tung University
1001 Ta Hsueh Road, Hsinchu 300 (Taiwan)

Prof. Dr. P. Leproux, Prof. Dr. V. Couderc
Institut de Recherche XLIM, UMR CNRS, No. 6172
123 avenue Albert Thomas, 87060 Limoges cedex (France)

Dr. J. P. R. Day, Prof. Dr. M. Bonn
Biosurface Spectroscopy
FOM Institute for Atomic and Molecular Physics
Science Park 104, 1098 XG Amsterdam (The Netherlands)

[**] This work was supported by the SENTAN project (Program-S) of the Japan Science and Technology Agency (JST). H. Kano gratefully acknowledges financial support from the Precursory Research for Embryonic Science and Technology (PRESTO) program of JST. The authors thank C. Onogi for providing the spontaneous Raman spectrum of yeast mitochondria, Leukos and Horus Laser companies for technical support, and Dr. F. Omura and H. Yomo (Suntory Co., Ltd.) for providing us with the yeast sample. We gratefully acknowledge J. Ukon (HORIBA, Ltd.) for assisting in the collaboration between the Japanese and French groups.

Supporting information for this article is available on the WWW under http://dx.doi.org/10.1002/anie.201001560.

CARS spectra at high speed. There is no need of scanning the laser wavelength or spectrometer in this method. Figure 1b shows the experimental setup (see details in the Supporting Information). We used a nanosecond white-light laser source excited by a sub-nanosecond microchip YAG laser for the broadband Stokes (ω_2) radiation (Figure 1c).

Figure 2a,b shows two fingerprint region CARS spectra obtained from two different positions in a living budding yeast cell (a zygote of *Saccharomyces cerevisiae* and *Saccharomyces bayanus*). By comparison with the known Raman spectra of yeast organelles, it is clear that the spectrum in Figure 2a is measured from the mitochondria and Figure 2b from the cytoplasm/nucleus. To the best of our knowledge, this is the first report of a fingerprint region CARS spectrum of a living cell at subcellular spatial resolution. The fact that a spectrum can be measured in tens of milliseconds allows us to follow the dynamics of cellular processes, as will be shown below. All the sharp peaks in Figure 2a,b originate from vibrational resonances. They show dispersive band shapes as a result of interference with the nonresonant background (NRB). This coherent nature of CARS enables us to extract the vibrationally resonant components by using the NRB as a local oscillator. In the present study, we employed the maximum entropy method (MEM) to extract the amplitude and phase of vibrational resonances from the obtained multiplex CARS spectra.[14] The MEM does not require any a priori knowledge of the vibrational bands contained but still is able to retrieve the phase information on the third-order nonlinear susceptibility $\chi^{(3)}$, whose imaginary part corresponds to ordinary (spontaneous) Raman spectra. Therefore, the amplitude of the retrieved band, Im[$\chi^{(3)}$], is proportional to the molecular concentration. In other words, each band can be evaluated quantitatively.

Figure 2c,d shows the Im[$\chi^{(3)}$] spectra converted by MEM from the CARS spectra in Figure 2a,b, respectively. It is clear that dispersive band shapes in Figure 2a,b are converted by MEM to normal band shapes. The wide applicability of MEM for retrieving vibrational resonances has already been demonstrated previously.[15–16] We further performed a singular value decomposition (SVD) analysis to reduce the noise in the retrieved Im[$\chi^{(3)}$] spectra.[17] The results are shown in Figure 2e,f. The signal-to-noise ratio is markedly improved on going from Figure 2c,d to Figure 2e,f. It should be emphasized that such SVD analysis cannot be applied to raw CARS spectra, because of their nonlinear nature. To perform noise filtering by SVD, retrieval of Im[$\chi^{(3)}$] spectra by MEM is indispensable. For comparison, Figure 2g shows a typical spontaneous Raman spectrum of yeast mitochondria in the same fingerprint region. It is evident that the MEM procedure correctly retrieves the Raman resonant components from the seemingly complex CARS spectrum.

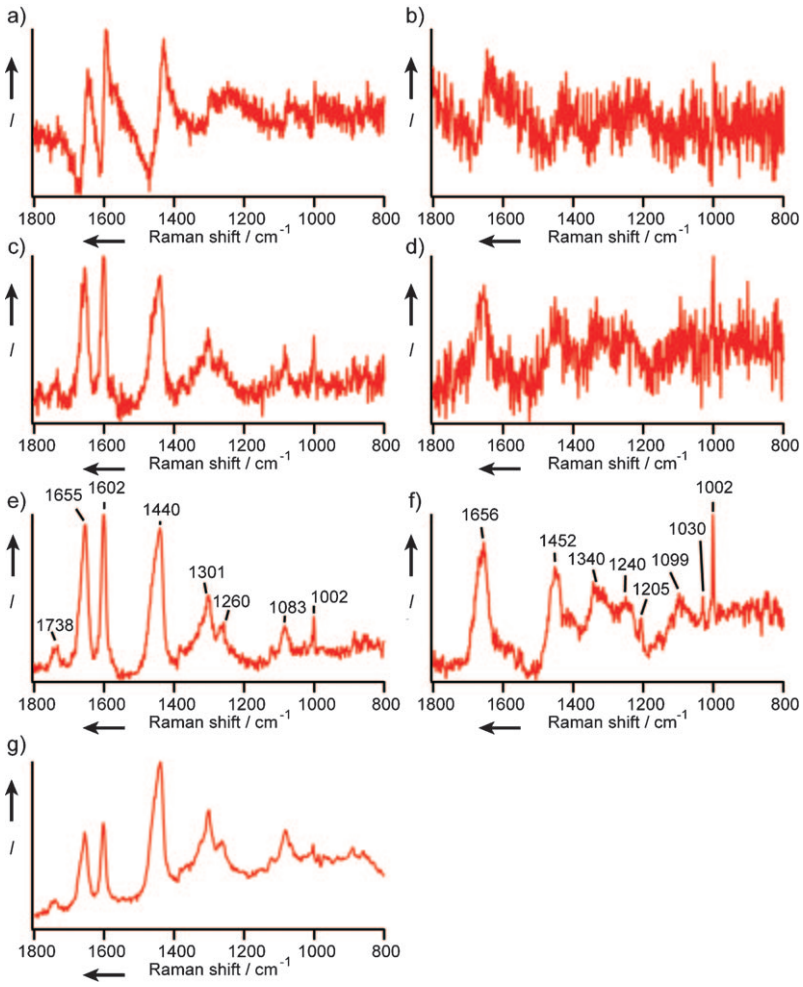

Figure 2. a,b) Typical CARS spectra in the fingerprint region of a living budding yeast cell; c,d) Im[$\chi^{(3)}$] spectra obtained by using MEM; e,f) Im[$\chi^{(3)}$] spectra after a SVD analysis; g) spontaneous Raman spectrum. The exposure time for measurement of the CARS and spontaneous Raman spectra was 50 ms and 300 s, respectively.

We shall now focus on the spectrum of mitochondrion in Figure 2e. The assignment has been reported in detail using spontaneous Raman microspectroscopy.[18] Briefly, the band at 1655 cm^{-1} is assigned to the superposition of the C=C stretch of lipid chains and the amide I mode of proteins. The band at 1440 cm^{-1} is assigned to the CH bend mode. This peak shows a slightly asymmetric band shape, because two CH bend modes, CH_2 scissors and CH_3 degenerate deformation, overlap. As is shown below, this band is decomposed into two bands originating from CH_2 and CH_3 in the present high resolution CARS measurements. The band at 1602 cm^{-1} shows unique properties that have been found in our previous studies.[18–19] This Raman band originates exclusively from mitochondria and its intensity sharply reflects the metabolic activity of mitochondria. We therefore call this band at 1602 cm^{-1} the "Raman spectroscopic signature of life".[19] Recently, we suggested the possibility of assigning this 1602 cm^{-1} band to the in-phase C=C stretch mode of ubisemiquinone, an electron carrier in the electron-transport chain in mitochondria,[20] on the basis of ^{13}C and ^{2}H

isotope substitution experiments. Figure 2e contains further detailed vibrational information; Raman bands at 1738, 1301, 1260 and 1083 cm^{-1} originate from the phospholipids that constitute mitochondria membranes.[19] The sharp band at 1002 cm^{-1} is assigned to the phenylalanine residues in proteins .[18] All these features in Figure 2e agree excellently with those in the corresponding spontaneous Raman spectrum (Figure 2g). MEM is thus proven to be a powerful technique to retrieve the correct $Im[\chi^{(3)}]$ spectra from congested CARS spectra over the entire spectral range of the fingerprint region. It enables us to use CARS spectra for quantitative molecular fingerprinting.

Next, we discuss the spectrum of the cytoplasm/nucleus in Figure 2f. This spectrum is totally different from that of the mitochondrion in Figure 2e. It has already been discussed that the band at 1002 cm^{-1} is assigned to phenylalanine, which is accompanied by the weak bands at 1205 and 1030 cm^{-1}. The high intensity of this band in Figure 2f indicates that protein molecules are predominantly located in the cytoplasm/nucleus. Accordingly, the bands at 1656, 1452, 1340, and 1240 cm^{-1} are assigned to amide I, CH bend, CH deformation, and amide III of proteins, respectively. It is noted that the peak position of the CH bend band in Figure 2f (1452 cm^{-1}) is different from that (1440 cm^{-1}) in Figure 2e. This frequency difference indicates that the contribution of CH_3 is larger than that of CH_2 in the CH bending band in Figure 2f. This result is consistent with proteins having a larger CH_3/CH_2 ratio than phospholipids. In addition to the band due to proteins, a nucleic acid band (symmetric stretching of PO_2^-) is also observed as a broad feature at 1099 cm^{-1}.

Figure 3a–l shows label-free and multifrequency (12 frequencies) $Im[\chi^{(3)}]$ images of a living budding yeast cell. Peak intensities were used for making these images. The exposure time for each pixel was 50 ms, and each image consists of 21 × 21 pixels. The overall measurement time was 22 sec. These images (a–l) were obtained simultaneously in one scan of the sample. As discussed, the CH bending band

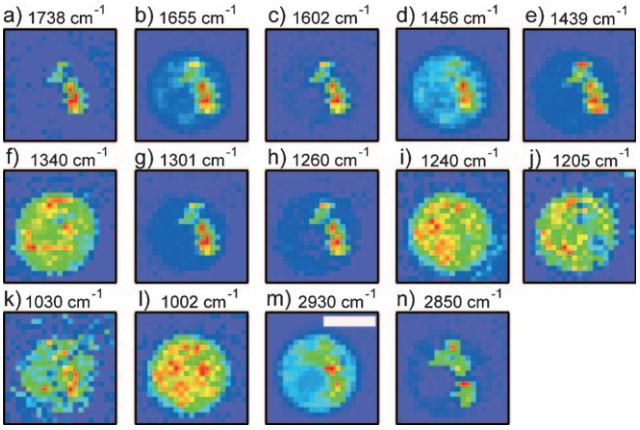

Figure 3. Label-free and multifrequency (14 frequencies) $Im[\chi^{(3)}]$ images of a living budding yeast cell at the Raman shift of 1738, 1655, 1602, 1456, 1439, 1340, 1301, 1260, 1240, 1205, 1030, and 1002 cm^{-1} (a–l). The scale bar in (m) is 4 μm. CARS images at the Raman shift of 2930 cm^{-1} (m) and 2850 cm^{-1} (n) are also indicated.

was successfully decomposed into two, the CH_3 degenerate deformation (d, 1456 cm^{-1}) and CH_2 scissors (e, 1439 cm^{-1}), respectively. For reference, CARS images at the Raman shift of 2930 cm^{-1} (m) and 2850 cm^{-1} (n) are also shown. These images were also simultaneously obtained by adjusting the center wavelength of spectrometer to the CH stretching region.

We can classify all the $Im[\chi^{(3)}]$ images in Figure 3 into three groups. The first group consists of the images in Figure 3a,c,e,g,h,n. They show localized and intense signal inside the cell. The second group contains the images in Figure 3f,i,j,k,l. These images show less heterogeneous molecular distributions inside the cell than those in the first group. The third group consists of Figure 3b,d,m. They look like the sum of the images of the first and second categories. The images of the first group except that of Figure 3c (1602 cm^{-1}) are ascribed to phospholipids, which are the main molecular species constituting mitochondria. The image Figure 3c (1602 cm^{-1}) coincides with the images of the phospholipids, reflecting that the "Raman spectroscopic signature of life" is localized at the mitochondria. In contrast, the images of the second group are assigned to proteins. The images of the third group correspond to the sum of images due to phospholipids and proteins. The band at 1655 cm^{-1} is the superposition of the C=C stretching of lipid chains and the amide I mode of proteins. The bands at 1456 and 2930 cm^{-1} originate from the CH_3 groups that are contained in both of phospholipids and proteins. Interestingly, the images in Figure 3d,e (CH bending) agree well with those in Figure 3m,n (CH stretching), respectively. There is therefore no need to acquire CARS images in the CH stretching region, which only contains part of the vibrational information also contained in the fingerprint region.

Since most of the single frequency CARS imaging so far has been performed at the CH stretch band, it would be useful to compare the signal-to-noise ratio (SNR) in the CH stretch region with that in the fingerprint region. On the basis of the result in Figure 3, we evaluated the SNR quantitatively. The ratio of the SNR of the CH_2 stretch band to that of the CH_2 bend band was calculated to be 4.7 under the present experimental conditions. Owing to the chromatic aberration, this value depends on how broad we measured the CARS spectrum. Figure 3 was obtained by optimizing the setup for the CARS measurement in the fingerprint region. We could therefore shorten the measurement time considerably by observing only the CH stretch band for imaging.

CARS molecular fingerprinting enables us to obtain label-free and multicolor images with high speed. Figure 4 shows the results of a real-time CARS study of a budding yeast cell over a time span of 35 min (a movie is available in Figure S3 in the Supporting Information. The CARS images at the CH stretch bands are also available). Four series of time-resolved images at the Raman shifts of 1655, 1602, 1446, and 1160 cm^{-1} are presented. The band at 1446 cm^{-1} corresponds to the overlap of the bands due to CH bend originating from CH_2 and CH_3. The band at 1160 cm^{-1} is obtained from a "dancing body" (DB) in a vacuole.[20] DBs are known to appear occasionally and move vigorously in a vacuole of a starving yeast cell. In our previous spontaneous Raman

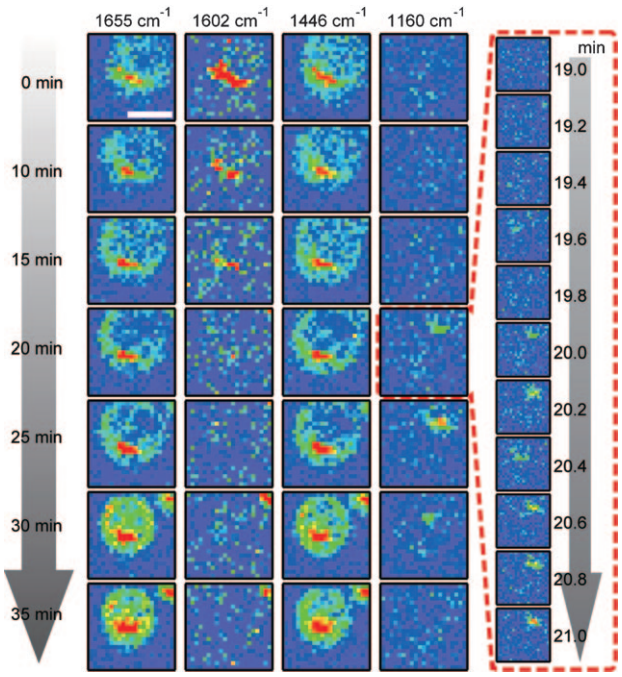

Figure 4. Time-resolved CARS images of the Raman bands at 1655 cm^{-1}, 1602 cm^{-1}, 1446 cm^{-1}, and 1160 cm^{-1}, respectively. The scale bar is 5 μm. The color scale for each band is the same for all the times measured. The red frame on the right contains CARS images at 1160 cm^{-1} from 19 to 21 min. Each image was measured every 12 s. Each of the 7 rows of images is constructed from Raman intensities retrieved from one CARS spectrum (movie is available in Figure S3 in the Supporting Information).

study,[21] it was found that DBs contain a high concentration of polyphosphate, which gives a Raman band at 1160 cm^{-1} assigned to the PO_2^- symmetric stretch mode. We traced the appearance of a DB and subsequent changes of the cell in Figure 4. At 0 min, the cell seems to be in a normal condition having active mitochondria shown by the bright 1602 cm^{-1} image. The intensity of the 1602 cm^{-1} band gradually decreases with time, although the intensities of the other bands do not show any appreciable changes between 0 and 15 min. At 20 min, the 1602 cm^{-1} band has almost disappeared, indicating that the metabolic activity in mitochondria has become minimal. Concomitantly, the polyphosphate band at 1160 cm^{-1} suddenly appears inside the vacuole. To trace this process more closely, time-resolved CARS images between 19 and 21 min are also shown in Figure 4 (highlighted by a red frame). The 1160 cm^{-1} band intensity gradually increases with time, showing the appearance of the DB in real time. At 21 min, the DB stops moving and stays at the upper part of the vacuole. At 30 min, the cell shrinks, and the vacuole disappears at the same time. The overall dynamic behavior inside the cell is interpreted in the following way. First, the metabolic activity in mitochondria is gradually lowered. At 20 min, the metabolic activity in mitochondria almost ceases, and subsequently a DB appears inside the vacuole. Finally, the DB is disrupted, and the cell shrinks at the same time. The cell is dead at this stage.

CARS microspectroscopy combined with MEM has realized label-free and quantitative molecular mapping of a single living cell in the fingerprint region (CARS molecular fingerprinting). It allowed us to obtain vibrational images with higher time resolution than that using conventional spontaneous Raman microscopy. Although the fingerprint region is spectrally congested in a living yeast cell, we were able to extract more than 10 vibrationally resonant $Im[\chi^{(3)}]$ images by MEM. This method was applied to a time-resolved study of dynamical processes in a single living yeast cell. It was found that the laser irradiation with about 20 mW power causes lowering and subsequent ceasing of the metabolic activity of mitochondria, followed by the appearance of a DB, and the eventual cell death in 35 min.

Rapid cell death such as that observed in the present study was never observed in our previous spontaneous Raman experiment, in which much lower laser power (4 mW) was used. In harmony with our previous observation of the starving death process, however, a clear correlation of the disappearance of the "Raman spectroscopic signature of life" to the appearance of a DB was found. It was also manifested by the change of the spectral profile (see Figure S2 in the Supporting Information). The present CARS experiment has shown clearly that the loss of the "Raman spectroscopic signature of life" precedes the formation of a dancing body. It is highly likely that the loss of metabolic activity in mitochondria causes, through an unknown mitochondria–vacuolar cross-talk, the formation of a DB in a vacuole. Our previous spontaneous Raman study was unable to address such details because of its low time resolution. We are now able to discuss quantitatively the life and death of a single cell at the molecular level.

The laser irradiation effect on the sample living cell has been examined by lowering the laser power. Dynamical changes of the distribution of organelles inside the cell were clearly observed but no perturbed cell behavior was noticeable with the 5 mW pump and 10 mW Stokes laser power (see Figure S1 in the Supporting Information).

In conclusion, CARS imaging has been improved to provide CARS molecular fingerprinting, which offers cellular biology a new strategic method that is complementary to optical and fluorescence microscopy.

Received: March 16, 2010
Revised: May 27, 2010
Published online: August 2, 2010

Keywords: CARS (coherent anti-Stokes Raman scattering) · time-resolved spectroscopy · vibrational spectroscopy

[1] A. Zumbusch, G. R. Holtom, X. S. Xie, *Phys. Rev. Lett.* **1999**, *82*, 4142.
[2] E. O. Potma, X. S. Xie, L. Muntean, J. Preusser, D. Jones, J. Ye, S. R. Leone, W. D. Hinsberg, W. Schade, *J Phys. Chem. B* **2004**, *108*, 1296.
[3] H. Kano, H. Hamaguchi, *Anal. Chem.* **2007**, *79*, 8967.
[4] G. J. Puppels, F. F. M. Demul, C. Otto, J. Greve, M. Robertnicoud, D. J. Arndtjovin, T. M. Jovin, *Nature* **1990**, *347*, 301.
[5] N. Dudovich, D. Oron, Y. Silberberg, *Nature* **2002**, *418*, 512.

[6] C. W. Freudiger, W. Min, B. G. Saar, S. Lu, G. R. Holtom, C. W. He, J. C. Tsai, J. X. Kang, X. S. Xie, *Science* **2008**, *322*, 1857.
[7] M. H. F. Kox, K. F. Domke, J. P. R. Day, G. Rago, E. Stavitski, M. Bonn, B. M. Weckhuysen, *Angew. Chem.* **2009**, *121*, 9152; *Angew. Chem. Int. Ed.* **2009**, *48*, 8990.
[8] M. D. Duncan, J. Reintjes, T. J. Manuccia, *Opt. Lett.* **1982**, *7*, 350.
[9] M. Hashimoto, T. Araki, S. Kawata, *Opt. Lett.* **2000**, *25*, 1768.
[10] B. N. Toleutaev, T. Tahara, H. Hamaguchi, *Appl. Phys. B* **1994**, *59*, 369.
[11] C. Otto, A. Voroshilov, S. G. Kruglik, J. Greve, *J. Raman Spectrosc.* **2001**, *32*, 495.
[12] M. Muller, J. M. Schins, *J. Phys. Chem. B* **2002**, *106*, 3715.
[13] J. X. Chen, A. Volkmer, L. D. Book, X. S. Xie, *J. Phys. Chem. B* **2002**, *106*, 8493.
[14] E. M. Vartiainen, *J. Opt. Soc. Am. B* **1990**, *7*, 722.
[15] E. M. Vartiainen, H. A. Rinia, M. Muller, M. Bonn, *Opt. Express* **2006**, *14*, 3622.
[16] G. I. Petrov, R. Arora, V. V. Yakovlev, X. Wang, A. V. Sokolov, M. O. Scully, *Proc. Natl. Acad. Sci. USA* **2007**, *104*, 7776.
[17] H. J. van Manen, Y. M. Kraan, D. Roos, C. Otto, *J. Phys. Chem. B* **2004**, *108*, 18762.
[18] Y. S. Huang, T. Karashima, M. Yamamoto, H. Hamaguchi, *Biochemistry* **2005**, *44*, 10009.
[19] Y. S. Huang, T. Karashima, M. Yamamoto, T. Ogura, H. Hamaguchi, *J. Raman Spectrosc.* **2004**, *35*, 525.
[20] C. Onogi, H. Torii, H. Hamaguchi, *Chem. Lett.* **2009**, *38*, 898.
[21] Y. Naito, A. Toh-e, H. Hamaguchi, *J. Raman Spectrosc.* **2005**, *36*, 837.

